



Discovery of SiO Masers in the "Water Fountain" Source IRAS 16552-3050

Downloaded from: <https://research.chalmers.se>, 2022-07-02 09:23 UTC

Citation for the original published paper (version of record):

Amada, K., Imai, H., Hamae, Y. et al (2022). Discovery of SiO Masers in the "Water Fountain" Source IRAS 16552-3050. *Astronomical Journal*, 163(2). <http://dx.doi.org/10.3847/1538-3881/ac3fb6>

N.B. When citing this work, cite the original published paper.



Discovery of SiO Masers in the “Water Fountain” Source IRAS 16552–3050

K. Amada¹ , H. Imai^{1,2,3} , Y. Hamae⁴, K. Nakashima⁴ , K. Y. Shum⁴, D. Tafoya⁵ , L. Uscanga⁶ , J. F. Gómez⁷ ,
G. Orosz^{8,9} , and R. A. Burns^{10,11}

¹ Graduate School of Science and Engineering, Kagoshima University, 1-21-35 Korimoto, Kagoshima 890-0065, Japan; k0501862@kadai.jp

² Amanogawa Galaxy Astronomy Research Center, Graduate School of Science and Engineering, Kagoshima University, 1-21-35 Korimoto, Kagoshima 890-0065, Japan

³ Center for General Education, Institute for Comprehensive Education, Kagoshima University, 1-21-30 Korimoto, Kagoshima 890-0065, Japan

⁴ Department of Physics and Astronomy, Faculty of Science, Kagoshima University, 1-21-35 Korimoto, Kagoshima 890-0065, Japan

⁵ Department of Space, Earth, and Environment, Chalmers University of Technology, Onsala Space Observatory, SE-439 92 Onsala, Sweden

⁶ Departamento de Astronomía, Universidad de Guanajuato, A.P. 144, 36000 Guanajuato, Gto., Mexico

⁷ Instituto de Astrofísica de Andalucía, CSIC, Glorieta de la Astronomía s/n, E-18008 Granada, Spain

⁸ School of Natural Sciences, University of Tasmania, Private Bag 37, Hobart, Tasmania 7001, Australia

⁹ Xinjiang Astronomical Observatory, Chinese Academy of Sciences, 150 Science 1-Street, Urumqi, Xinjiang 830011, People’s Republic of China

¹⁰ National Astronomical Observatory of Japan, 2-21-1 Osawa, Mitaka, Tokyo, 181-8588, Japan

¹¹ Korea Astronomy and Space Science Institute, 776 Daedeokdae-ro, Yuseong-gu, Daejeon 34055, Republic of Korea

Received 2021 June 21; revised 2021 November 30; accepted 2021 December 1; published 2022 January 24

Abstract

In this paper, we report new detections of SiO $v = 1$ and $v = 2$ $J = 1 \rightarrow 0$ masers in the “water fountain” source IRAS 16552–3050, which was observed with the Nobeyama 45 m telescope during 2021 March–April. Water fountains are evolved stars whose H₂O maser spectra trace high-velocity outflows of >100 km s^{−1}. This is the second known case of SiO masers in a water fountain, after their prototypical source, W 43A. These SiO masers should shed light on the evolutionary status of this category of evolved stars, which are likely to be at the end of the asymptotic giant branch phase, when the star exhibits the most copious stellar mass loss, followed by development of the complicated morphologies of planetary nebulae. The origin of a large (up to 25 km s^{−1}) velocity offset of the SiO masers with respect to the systemic velocity derived from the spectrum of CO $J = 2 \rightarrow 1$ line is discussed here.

Unified Astronomy Thesaurus concepts: Astrophysical masers (103); Silicon monoxide masers (1458); Stellar jets (1607); Stellar mass loss (1613); Asymptotic giant branch stars (2100)

1. Introduction

“Water fountain” (WF) sources are dying stars in the asymptotic giant branch (AGB) or post-AGB phases that show bipolar jets traced by H₂O maser emission (e.g., Imai 2007). These sources are usually identified from the presence of high-velocity components in their H₂O maser spectra, tracing motions significantly faster than the expansion of circumstellar envelopes around AGB stars (typically 10–20 km s^{−1}, e.g., Engels & Bunzel 2015). To date, 15 WFs have been confirmed (e.g., Gómez et al. 2017). Interestingly, the WFs exhibit a wide variety in the spatiokinematics of their H₂O masers as summarized in Imai et al. (2020). Recent molecular line observations of the WFs have suggested that the central stellar system is probably a binary forming a common envelope (e.g., Tafoya et al. 2020; Khouri et al. 2021). However, the evolutionary status of WFs in the context of stellar evolution is still mostly unknown due to the limited information on the vicinities of their central systems.

SiO maser emission is one of the key probes of the status of the stellar mass loss as seen in objects in the AGB phase and, in a limited number of cases, in the post-AGB phase (e.g., Gonidakis et al. 2013). To date, the presence of SiO masers has been confirmed in only one WF, W 43A (Nakashima & Deguchi 2003). Imai et al. (2005) mapped the W 43A SiO $v = 1$ $J = 1 \rightarrow 0$ masers, exhibiting a biconical outflow with a

wide full opening angle ($\sim 40^\circ$). The presence of SiO maser emission, together with the periodic variation of the OH masers at 1612 MHz (Herman & Habing 1985), provide strong evidence that the central system hosts an AGB star with a high mass-loss rate (see Tafoya et al. 2020). Note that the W 43A SiO masers have vanished recently as mentioned later.

In this paper, we report new detections of SiO masers in IRAS 16552–3050 (hereafter abbreviated as I16552). The distance to I16552 was estimated to be in $D = 8.4 \pm 1.7$ kpc through spectral energy distribution model fitting (Vickers et al. 2015). Figure 1 shows the WISE multi-band (3.4, 4.6, and 11.6 μ m) image toward I16552, available via the WISE Image Service. I16552 was identified as a WF by Suárez et al. (2007) and its H₂O masers were mapped by Suárez et al. (2008). The spatiokinematics of the H₂O masers exhibit a fast bipolar outflow with a wide opening angle. The IRAS colors of I16552 are consistent with those of an AGB star (Suárez et al. 2008), similar to the case of W 43A. However, it has been classified as a post-AGB star based on optical spectra (Suárez et al. 2006). In fact, no OH maser emission was found (Hu et al. 1994) although this is common among AGB stars. We further discuss the properties of the discovered SiO masers and their implications in terms of stellar mass-loss activity in later sections.

2. Observations

2.1. FLASHING (Nobeyama 45 m Telescope)

Using the Nobeyama 45 m telescope, we have observed all 14 WFs within reach of the telescope (including I16552 and W 43A), except IRAS 15103–5754, from 2018 December to

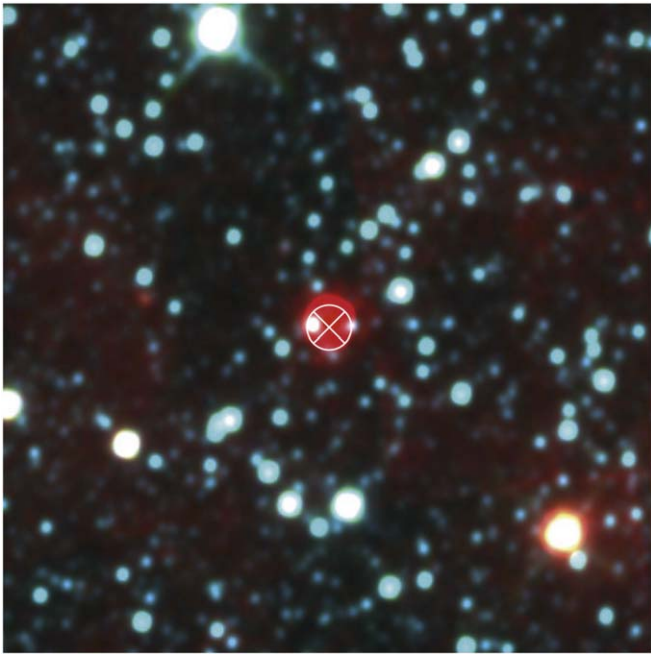


Figure 1. WISE multi-band image of the field around IRAS 16552–3050 in an area of $10' \times 10'$. The wavelength of the blue, green, and red images corresponds to 3.4, 4.6, and $22 \mu\text{m}$, respectively. The field center is at (J2000.0)(R.A., decl.) = ($16^{\text{h}}58^{\text{m}}27^{\text{s}}.31$, $-30^{\circ}55'07''.9$). A cross indicates the field center, corresponding to the pointing position of the Nobeyama 45 m telescope toward IRAS 16552–3050 (the central red object). A circle around the cross indicates the beam size of the telescope ($41''$ at 43 GHz).

2021 April in the FLASHING (Finest Legacy Acquisitions of SiO-/H₂O-maser Ignitions by Nobeyama Generation, Imai et al. 2020) project, in which 22 GHz H₂O and 43 GHz SiO masers are simultaneously monitored using the H22 and H40 receivers, respectively (Okada et al. 2020). This configuration allows us to search for the H₂O maser emission in the transition $J_{K,K^+} = 6_{12} \rightarrow 5_{23}$ at 22.235080 GHz and SiO maser emissions in the rotational transitions $J = 1 \rightarrow 0$ at the vibrational states $\nu = 0$ to 3 at 43 GHz. This paper mainly focuses on the SiO maser emissions of $\nu = 1$ and $\nu = 2$ at the rest frequencies of 42.82053 GHz and 43.122027 GHz, respectively, which were detected in I16552. All the signals received in the present observations were processed with the SAM45 spectrometer. For the SiO transitions, this backend provided a total bandwidth of 125 MHz with a spectral resolution of 61 kHz for each observed transition. This corresponds to a velocity coverage and resolution of 869 and 0.43 km s^{-1} for the $\nu = 1$ line, and 875 and 0.44 km s^{-1} for the $\nu = 2$ line.

I16552 was observed in 16 epochs, each for about 20 minutes using the H40 receiver, in left-hand circular polarization, with a typical system temperature of 250 K for the source elevation of $\sim 22^\circ$. The pointing position of the Nobeyama 45 m telescope toward I16552 was (J2000.0)(R.A., decl.) = ($16^{\text{h}}58^{\text{m}}27^{\text{s}}.31$, $-30^{\circ}55'07''.9$). After the SiO maser detection in 2021 March, I16552 was observed for about one hour in each epoch using the Z45 receiver (Nakamura et al. 2015) alone, which can receive signals of two orthogonal linear polarization paths with lower system temperatures ($T_{\text{sys}} \sim 230 \text{ K}$ and $\sim 170 \text{ K}$ on April 13 and 27, respectively). The backend and spectral setup with Z45 were the same as that with H40 described above.

Table 1
Record of the FLASHING Observations of the SiO Masers in
IRAS 16552–3050

Date (YYYY-MM-DD)	T_{sys} (K)		Noise (mJy) ^a	
	$\nu = 1$	$\nu = 2$	$\nu = 1$	$\nu = 2$
2019-01-03	313	234	156	108
2019-02-20	234	230	158	149
2019-03-06	254	247	230	214
2019-04-27	1358	1337	720	700
2019-05-30	255	250	117	110
2019-12-06	268	299	184	194
2020-02-07	256	260	212	219
2020-03-07	295	297	197	203
2020-03-21	259	282	177	183
2020-04-16	242	270	179	196
2020-12-23	227	233	144	140
2021-01-06	243	249	150	143
2021-01-19	237	243	140	140
2021-03-19	251	260	155	152
2021-03-31	292	304	167	176
2021-04-13	260, 251 ^b	273, 230 ^b	230, 97 ^c	234, 80 ^c
2021-04-27	260, 170 ^b	271, 151 ^b	232, 53 ^c	233, 44 ^c

Notes. The boldface is the date when SiO maser was detected.

^a rms noise level before channel smoothing (velocity resolution of 0.43 and 0.44 km s^{-1} in the SiO $\nu = 1$ and $\nu = 2$ spectra, respectively).

^b The system noise temperatures of the observations using the H40 and Z45 receivers, respectively.

^c rms noise levels of the observations using the H40 and Z45 receivers, respectively, before spectral smoothing.

Data reduction was carried out using the¹² JavaNewstar package in a standard manner, namely, data integration in the time domain followed by spectral baseline fitting in the maser emission-free spectral channels. Table 1 gives a summary of the monitoring observations of I16552 in 16 epochs: the dates of the observation epochs and the yielded root-mean-square (rms) noise levels of the obtained SiO maser spectra before spectral smoothing. Here a conversion factor of 3.2 Jy K^{-1} was adopted to convert the antenna temperature to the flux density scale. A 3σ detection limit to the SiO masers was typically $\leq 300 \text{ mJy}$ in the spectrum with velocity resolution 1.72 km s^{-1} and 1.76 km s^{-1} for the $\nu = 1$ and $\nu = 2$, respectively, after four-channel smoothing for the spectrum taken with the H40 receiver. Similarly, W43A was also inspected but with no detection of SiO masers in all epochs. In our discussion, we will also present, for comparison, one of the H₂O maser spectra of I16552 taken within the FLASHING project. The presented spectrum is taken from the observation on 2021 March 19 when the masers covered the greatest velocity range (from $V_{\text{LSR}} = -79$ to 128 km s^{-1}). For the H₂O maser spectrum, a conversion factor 2.8 Jy K^{-1} was adopted. For this transition, we used the SAM45 spectrometer, with a bandwidth of 62 MHz (842 km s^{-1}) and a spectral resolution of 31 kHz (0.41 km s^{-1}).

2.2. ALMA

I16552 was also observed in the CO ($J = 2 \rightarrow 1$) line at 230.538 GHz with the Atacama Large Millimeter-submillimeter Array (ALMA) on 2019 January 18. The integration time of ~ 11 minutes yielded an rms noise level of 3 mJy in the

¹² <https://www.nro.nao.ac.jp/~nro45mrt/html/obs/newstar/>

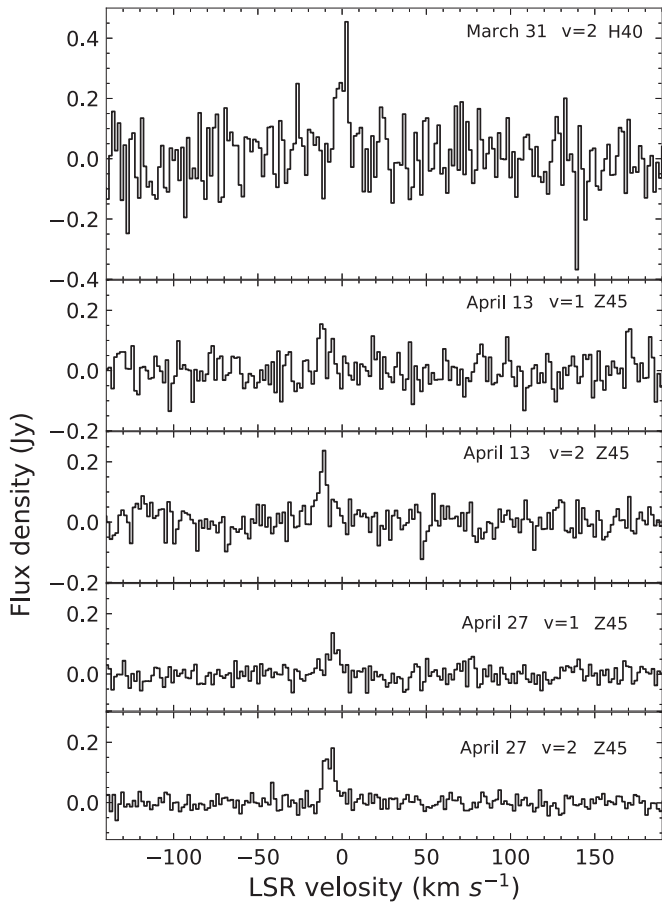


Figure 2. Spectra of SiO $\nu = 1$ and $\nu = 2$ ($J = 1 \rightarrow 0$) masers in IRAS 16552–3050. The spectra were obtained after smoothing in four consecutive spectral channels. The spectra taken with H40 (on 2021 March 31) and Z45 (on 2021 April 13 and 27) with firm maser detections are displayed.

spectrum with a bandwidth of 938 MHz (1219 km s^{-1} in a velocity resolution 1.5 km s^{-1}) and a synthesized beam of $1''.24 \times 1''.18$ at a position angle of -78° . This paper shows only the CO spectrum in order to estimate the systemic velocity of I16552, while the whole results of the ALMA observation will be published in a separate paper.

3. Results and Discussion

Figure 2 shows the spectra of the SiO $\nu = 1$ and $\nu = 2$ masers detected on 2021 March 31 and April 13 and 27. The first detection of the SiO masers was confirmed only in the $\nu = 2$ line on March 31. The detections of both the $\nu = 1$ and $\nu = 2$ masers were confirmed with the Z45 receiver in higher sensitivity observations on April 13 and 27. Table 2 gives the parameters of the detected SiO masers. Our criterion for determining a bona fide maser detection is that, after spectral smoothing, it shows a peak signal-to-noise ratio (S/N) higher than 5, or higher than 3, but over more than one consecutive spectral channel. Further confirmation can be obtained from comparing the spectral profiles among the different epochs (for the $\nu = 2$ line) and between the $\nu = 1$ and $\nu = 2$ lines (on April 13 and 27). This is the reason why we consider the maser $\nu = 1$ on April 13 to be a clear detection. The variation of the velocities at the spectral peaks is likely attributed to thermal noise’s wander. Such a wander is significant in the $\nu = 2$ spectrum on March 31 with a low S/N. On April 27 we

Table 2
Parameters of SiO Masers in IRAS 16552–3050

Date (2021)	S_{peak} (mJy) ^a		$V_{\text{LSR}}^{\text{peak}}$ (km s^{-1}) ^b		RX ^c
	$\nu = 1$	$\nu = 2$	$\nu = 1$	$\nu = 2$	
Mar 31		454 (5.0)		3.5	H40
Apr 13	154 (3.0)	237 (6.0)	−11.5	−9.9	Z45
Apr 27	136 (5.3)	181 (8.2)	−4.7	−4.7	Z45
		144 (6.5)		−8.2	

Notes.

^a Peak flux density of the SiO maser, and the signal-to-noise ratio of the maser detection in parentheses. The signal-to-noise ratio was calculated using the rms obtained after four-channel smoothing, reduced by a factor of two from that given in Table 1.

^b LSR velocity at the peak of the detected maser line.

^c Used receiver.

detected one SiO maser, but its spectral profile suggests that the maser might be composed of two blending features. This profile also can be noted in the spectrum on April 13 where the feature at a higher velocity is below the detection threshold. For the rest of the discussion, we will consider the maser on April 27 to be composed of two separate maser features.

Although SiO masers in the rotational transitions of $J = 1 \rightarrow 0$ are found in massive star-forming regions, only seven such SiO maser emitters have been confirmed (Cho et al. 2016; Cordiner et al 2016). They are distinguishable from other SiO masers associated with long-period variable evolved stars because the former is basically stable while the latter shows periodicity synchronized with the stellar light curve (e.g., Pardo et al. 2004). Note that Yoon et al. (2014) reported negative detection of the SiO masers in their observations of I16552 on 2011 February 23 below a relatively high detection threshold (a 3σ upper limit of 1.3 Jy). Therefore, it is difficult to further discuss the temporal variability in the SiO masers in I16552. AGB and post-AGB stars are bright in the mid- and far-infrared. Within the beam of our observations, there are 10 near-infrared sources in the 2MASS point source catalog (Skrutskie et al. 2006) and 84 optical sources in the GAIA EDR3 catalog (Gaia Collaboration et al. 2016, 2021). However, WISE images (Figure 1) clearly show that the pointing position of the Nobeyama observations corresponds to a red source, which is very bright at the WISE bands of longer wavelength. This is the counterpart of the IRAS source, and it must be the source hosting the SiO masers we report here.

The SiO masers are blueshifted by $\sim 25 \text{ km s}^{-1}$ from the systemic velocity, $V_{\text{LSR}} \sim 16 \text{ km s}^{-1}$, which is determined from the spectrum of the CO $J = 2 \rightarrow 1$ emission obtained with ALMA in I16552 as shown in Figure 3. This velocity offset is comparable to, but slightly larger than, those in W 43A and Orion Source I, a massive young star ($\sim 20 \text{ km s}^{-1}$, Imai et al. 2005; Matthews et al. 2009). In W 43A, the SiO masers exhibited biconical expansion at a velocity greater than that of the 1612 MHz OH masers ($\sim 8 \text{ km s}^{-1}$) but less than that of H₂O masers ($\sim 150 \text{ km s}^{-1}$, Imai et al. 2002). This supports a model in which the SiO masers were associated with the jet’s nozzles formed in entrained material dragged by the fast jet (Tafuya et al. 2020). In fact, the velocities of the SiO masers corresponded to the spectral edge of the CO emission. The SiO masers in I16552 may resemble the case of W 43A, but it should be confirmed in future observations, for instance, by

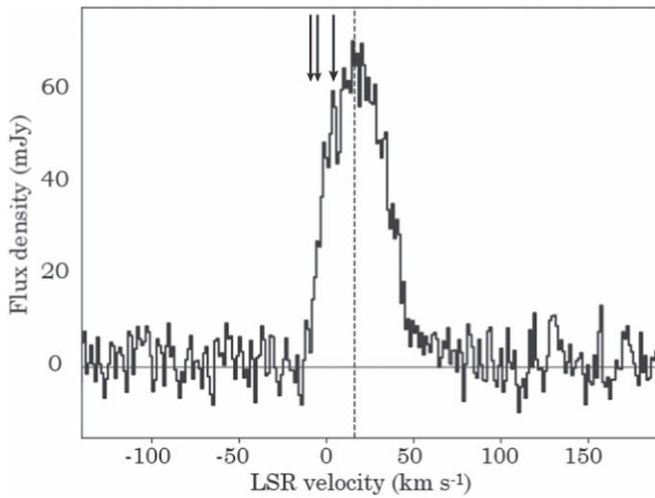


Figure 3. Spectrum of CO ($J=2 \rightarrow 1$) emission in IRAS 16552–3050. A vertical dashed line indicates the systemic velocity of the source, $v_{\text{sys}} = 16 \text{ km s}^{-1}$. Vertical arrows indicate the velocities of the detected SiO masers around $V_{\text{LSR}} \sim -9, -5, \text{ and } 4 \text{ km s}^{-1}$.

finding the expected redshifted counterpart SiO masers and by spatially locating these masers.

Figure 4 shows one of the H₂O maser spectra of I16552 taken recently in FLASHING. We note that the total velocity coverage of this H₂O maser emission has expanded: from an LSR velocity range of $V_{\text{LSR}} = -70$ to 115 km s^{-1} in 2005 September (Suárez et al. 2007, 2008; Yoon et al. 2014) to the latest one of -79 to 128 km s^{-1} in 2021 March. Due to a lack of estimation of the dynamical age of the jet in I16552, it is difficult to discuss a physical link between the new discovery of the SiO masers and the expansion of the velocity coverage of H₂O masers although the latter can be considered a recent launch of the faster jet as proposed for IRAS 18286–0959 by Imai et al. (2020).

The SiO masers in WFs such as W 43A and I16552 shed light on the evolution of WFs with a wide variety of the spatiokinematics of H₂O masers and that of the physical conditions indicated in the combination of excited maser lines. W 43A was the only known WF hosting SiO masers. Taking into account its possible association with an AGB star mentioned in Section 1, SiO masers in WFs could be associated with a star whose jet’s dynamical age is still very short ($<100 \text{ yr}$, Tafuya et al. 2020) and relics of the circumstellar envelope still remain in the vicinity of the central stellar system. However, the detections of SiO masers in I16552, a post-AGB star, require reconsideration on such a model of the evolutionary status of WFs hosting SiO masers. Note that SiO masers are also hosted by the pre-planetary nebula OH 231.8 +4.2 (Kim et al. 2019 and references therein). Their characteristics look very similar to those in AGB stars including their periodic variation. SiO masers around AGB and post-AGB stars may be commonly understandable. Another common property of these stars is that the spatiokinematics of H₂O masers have clear bipolarity (Imai et al. 2002; Suárez et al. 2008; Dodson et al. 2018). After mapping and spatially locating the SiO masers with radio interferometric observations and testing for the maser excitation model in I16552 mentioned above, we will be able to construct an evolution model of the stellar mass loss driven by the jet hosting H₂O masers and its biconical nozzles hosting SiO masers.

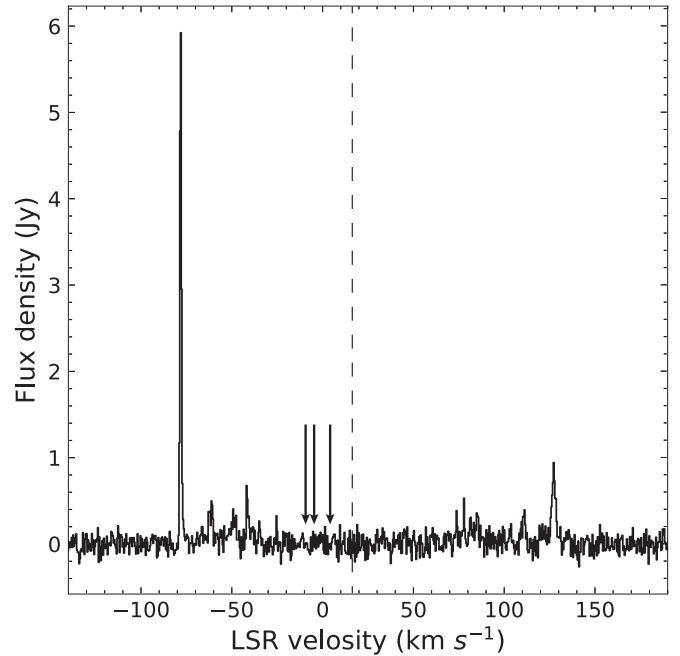


Figure 4. Spectrum of the H₂O maser emission observed on 2021 March 19 when the masers recently covered the greatest velocity range (from $V_{\text{LSR}} = -79$ to 128 km s^{-1}). The rms noise level of the spectrum is 95 mJy . The vertical dashed line and vertical arrows are the same as those in Figure 3.

The Nobeyama 45 m radio telescope is operated by Nobeyama Radio Observatory, a branch of the National Astronomical Observatory of Japan (NAOJ), National Institutes of Natural Sciences. We used the data taken in the project 2018.1.00250.S of ALMA, which is a partnership of ESO (representing its member states), NSF (USA) and NINS (Japan), together with NRC (Canada), NSC and ASIAA (Taiwan), and KASI (Republic of Korea), in cooperation with the Republic of Chile. The Joint ALMA Observatory is operated by ESO, AUI/NRAO, and NAOJ. This publication also makes use of data products from the Wide-field Infrared Survey Explorer, which is a joint project of the University of California, Los Angeles, and the Jet Propulsion Laboratory/California Institute of Technology, funded by the National Aeronautics and Space Administration. H.I. is supported by JSPS KAKENHI grant No. JP 16H02167. J.F.G. acknowledges support from the State Agency for Research (AEI/10.13039/501100011033) of the Spanish MCIU, through grant PID2020-114461GB-I00 and the “Center of Excellence Severo Ochoa” award for the Instituto de Astrofísica de Andalucía (SEV-2017-0709).

Facilities: NRO 45 m telescope, ALMA, SIMBAD, WISE Image Service (IRSA).

Software: JavaNewstar (<https://www.nro.nao.ac.jp/~nro45mrt/html/obs/newstar/>); Kinematic Distance Calculation Tool (<https://www.treywenger.com/kd/>).

ORCID iDs

- K. Amada <https://orcid.org/0000-0003-4419-6132>
H. Imai <https://orcid.org/0000-0002-0880-0091>
K. Nakashima <https://orcid.org/0000-0002-8764-9595>
D. Tafuya <https://orcid.org/0000-0002-2149-2660>
L. Uscanga <https://orcid.org/0000-0002-2082-1370>
J. F. Gómez <https://orcid.org/0000-0002-7065-542X>
G. Orosz <https://orcid.org/0000-0002-5526-990X>

R. A. Burns  <https://orcid.org/0000-0003-3302-1935>

References

- Cho, S.-H., Yun, Y., Kim, J., et al. 2016, *ApJ*, **826**, 157
- Cordiner, M. A., Boogert, A. C. A., Charnley, S. B., et al. 2016, *ApJ*, **828**, 51
- Dodson, R., Rioja, M., Bujarrabal, V., et al. 2018, *MNRAS*, **476**, 520
- Engels, D., & Bunzel, F. 2015, *A&A*, **582**, A68
- Gaia Collaboration, Prusti, T., de Bruijne, J. H. J., et al. 2016, *A&A*, **595**, A1
- Gaia Collaboration, Brown, A. G. A., Vallenari, A., et al. 2021, *A&A*, **649**, A1
- Gómez, J. F., Suárez, O., Rizzo, J. R., et al. 2017, *MNRAS*, **468**, 2081
- Gonidakis, I., Diamond, P. J., & Kemball, A. J. 2013, *MNRAS*, **433**, 3133
- Herman, J., & Habing, H. J. 1985, *A&AS*, **59**, 523
- Hu, J. Y., te Lintel Hekkert, P., Slijkhuis, F., et al. 1994, *A&AS*, **103**, 301
- Imai, H. 2007, in *IAU Symp. 242, Astrophysical Masers and their Environments*, ed. W. Baan & J. Chapman (Cambridge: Cambridge Univ. Press), 279
- Imai, H., Nakashima, J., Diamond, P. J., Miyazaki, A., & Deguchi, S. 2005, *ApJL*, **622**, L125
- Imai, H., Obara, K., Diamond, P. J., Omodaka, T., & Sasao, T. 2002, *Natur*, **417**, 829
- Imai, H., Uno, Y., Maeyama, D., et al. 2020, *PASJ*, **72**, 58
- Khoury, T., Vlemmings, W. H. T., Tafuya, D., et al. 2021, *NatAs*, in press
- Kim, J., Cho, S.-H., & Bujarrabal, V. 2019, *MNRAS*, **488**, 1427
- Matthews, L. D., Greenhill, L. J., Goddi, C., et al. 2009, *ApJ*, **708**, 80
- Nakamura, F., Ogawa, H., Yonekura, Y., et al. 2015, *PASJ*, **67**, 117
- Nakashima, J., & Deguchi, S. 2003, *PASJ*, **55**, 229
- Okada, N., Hashimoto, I., Kimura, K., et al. 2020, *PASJ*, **72**, 7
- Pardo, J. R., Alcolea, J., Bujarrabal, V., et al. 2004, *A&A*, **424**, 145
- Skrutskie, M. F., Cutri, R. M., Stiening, R., et al. 2006, *AJ*, **131**, 1163
- Suárez, O., Gómez, J. F., & Miranda, L. F. 2008, *ApJ*, **689**, 430
- Suárez, O., Gómez, J. F., & Morata, O. 2007, *A&A*, **467**, 1085
- Suárez, O., García-Lario, P., Manchado, A., et al. 2006, *A&A*, **458**, 173
- Tafuya, D., Imai, H., Gómez, J. F., et al. 2020, *ApJL*, **890**, L14
- Vickers, S. B., Frew, D. J., Parker, Q. A., & Bojičić, I. S. 2015, *MNRAS*, **447**, 1673
- Yoon, D.-H., Cho, S.-H., Kim, J., Yun, Y. J., & Park, Y.-S. 2014, *ApJS*, **211**, 15